*Aleksandar Petričević[1], Vladimir D. Jović[2], Mila N. Krstajić Pajić[1], Piotr Zabinski[3], Nevenka R. Elezović[2]**

[1]University of Belgrade, Faculty of Technology and Metallurgy, Belgrade, Serbia, [2]University of Belgrade, Institute for Multi-disciplinary Research, Belgrade, Serbia, [3]AGH University of Science and Technology, Faculty of Non-Ferrous Metals, Krakow, Poland

Scientific paper
ISSN 0351-9465, E-ISSN 2466-2585
https://doi.org/10.5937/zasmat2202153P

Zastita Materijala 63 (2)
153 - 164 (2022)

Oxygen reduction reaction on electrochemically deposited sub-monolayers and ultra-thin layers of Pt on $(Nb\text{-}Ti)_2AlC$ substrate

ABSTRACT

Catalytic activity towards the oxygen reduction reaction (ORR) in 0.5 M H_2SO_4 was investigated at sub-monolayers and ultra-thin layers (corresponding to 10, 30 and 100 monolayers, (MLs)) of Pt electrochemically deposited on $(Nb\text{-}Ti)_2AlC$ substrate. Electrochemical deposition of Pt layers on $(Nb\text{-}Ti)_2AlC$ substrate was achieved from the solution containing 3 mM K_2PtCl_4 + 0.5 M NaCl (pH 4) under the conditions of convective diffusion (RPM = 400) using linear sweep voltammetry (LSV) at a sweep rate of 2 mV s^{-1}, by determining limiting potential for deposition of each Pt sample from the Q_{Pt} vs. E curves. The Pt samples were characterized X-ray photoelectron spectroscopy (XPS). XPS analysis showed that practically the whole surface of $(Nb\text{-}Ti)_2AlC$ substrate is covered with homogeneous layer of Pt, while Pt ion reduction was complete to metallic form – Pt(0) valence state. Then oxygen reduction was studied at rotating disc electrode by cyclic voltammetry and linear sweep voltammetry. Two different Tafel slopes were observed, one close to 60 mV dec^{-1} in low current densities region and second one ~ 120 mV dec^{-1} in high current densities region. This novel catalyst exhibited higher activity in comparison to carbon supported one, in terms of mass activity – kinetic current density normalized to Pt loading.

Keywords: *Platinum electrodeposition, oxygen reduction, acid solution.*

1. INTRODUCTION

Pt is known as one of the best one-component catalyst for reactions taking place in fuel cells, as well as for many other technologically important reactions [1, 2].

Electrochemical deposition of one, ore more MLs of Pt for above mentioned applications are of great importance, due to high cost of Pt. Unfortunately, in order to understand initial stages of this process, Pt was electrodeposited on other noble metals, mainly on Au, Pd and Ru [3-31] by different techniques: by electrochemical deposition (at a constant potential or current) on Au [3-6] and Ru [7]; by spontaneous deposition on single crystalline [25-27] and polycrystalline Au [28], as well as on carbon-supported Au nanoparticles [29] and on Ru [7,11,24,30]; by redox replacement of Cu UPD monolayer on Au and Pd [8-22] and thin layers of Ni electrodeposited on Au [23].

In a few cases HOPG was used as a substrate for electrochemical deposition of Pt nanoclusters [7-9]. It was discovered that the process of Pt electrochemical deposition on Au(111) commences with the adsorption of ordered structures of $[PtCl_4]^{2-}$ and $[PtCl_6]^{2-}$ complexes (in situ STM investigations [25,31]). The second stage of Pt electrochemical deposition was the formation of incomplete 2D Pt deposit followed by 3D nucleation and growth of 3D nuclei, first on the monoatomic steps and later on the terraces [3,4]. Spontaneous deposition also resulted in a formation of incomplete 2D Pt layers [26-29], while the redox replacement [8-23], although providing almost complete Pt MLs, was considered as a complex procedure. Electrochemical deposition of Pt on graphite-based surfaces was studied [32-34]. It was referred that 3D growth of deposited platinum appeared to be the dominant mechanism. Various morphologies of Pt electrodeposition on HOPG were the consequence of competing between 3D and 2D particles growth [34]. A common conclusion for the process of Pt electrochemical deposition is that the formation of a complete, close-packed monolayer wasn't detected. Usually, potentials applied in these investigations were limited by the

*Corresponding author: Nevenka R. Elezović
E-mail: nelezovic@tmf.bg.ac.rs

Paper received: 08. 11. 2021.
Paper accepted: 10. 01, 2022.
Paper is available on the website: www.idk.org.rs/journal

beginning of UPD of hydrogen on Pt (H_{UPD}), while in the case of Pt electrochemical deposition from a pH 10 (electrolyte containing $NaHPO_4$ + $Pt(NH_3)_2(H_2O_2)_2^{2+}$) it was discovered that Pt electrochemical deposition was inhibited when the potential was scanned into the H_{UPD} region [35]. Following these results, Y. Liu et al. [36] investigated self-terminating growth of Pt on Au at room temperature in aqueous solutions containing 3 mM K_2PtCl_4 + 0.5 M NaCl, with pH values ranging between 2.5 and 4. It was demonstrated that during the potential pulse from 0.4 V vs. SSCE (sodium chloride saturated calomel electrode) to -0.8 V vs. SSCE the formation of a saturated H_{UPD} layer induces self-terminating effect on Pt electrochemical deposition, restricting it to a high coverage of 2D Pt islands. During the second potential pulse H_{UPD} layer is oxidized providing sequential deposition of Pt layers. After each pulse, independently of its duration (1 to 1000 s), one discrete 2D Pt layer was deposited. This was confirmed by EQCM and XPS measurements, while maximum number of pulses was 10. This effect was detected at the conditions of non-stationary and convective diffusion.

Recently, the same, self-terminating Pt electrochemical deposition process was used for a formation of catalytically active surface composed of Ni and Pt [37]. It was found by ion scattering spectroscopy (ISS) that Pt covered 60% of the Ni surface forming a $Pt_{50}Ni_{50}$ surface alloy. Electrochemical deposition of Pt on Ni by several cycles was complicated by emersion and rapid water rinsing in air to oxidize the H_{UPD} followed by re-immersion for additional electrochemical Pt deposition. The Pt-terminated surface was obtained after four such cycles. The HER and HOR in alkaline media were significantly enhanced on the Pt/Ni monolayer film relative to Pt monolayer. The Pt/Ni electrode showed deactivation with time [37].

In this work, following our earlier research on electrochemical deposition of thin layers of noble metals (Ru [38], Pd [39] and Ir [40,41]) on Ti_2AlC substrate (MAX phase) and their use as cathodes for the hydrogen evolution reaction (HER) in acid media, ultra-thin layers (10, 30 and 100 MLs) of Pt were electrochemically deposited on $(Nb\text{-}Ti)_2AlC$ substrate and the process of the ORR was investigated on such electrodes in sulfuric acid.

2. EXPERIMENTAL

All solutions were prepared using 18.2 MΩcm deionized water (Smart2PureUV, TKA) and p.a. chemicals (SIGMA-Aldrich), while all experiments were performed by using potentiostat Refrence 600 (Gamry Instruments, Inc.).

2.1. Electrochemical deposition of Pt

Electrochemical deposition of Pt was carried out in a standard three-electrode cell at room temperature, with Pt counter electrode and reference, saturated calomel electrode (SCE), being placed in separate compartments. SCE was placed in a side compartment connected to the main one through a bridge and a Luggin capillary. Electrochemical deposition of Pt on $(Nb\text{-}Ti)_2AlC$ substrate has been achieved from the solution containing x mM K_2PtCl_4 + 0.5 M NaCl (pH 4), previously purged with high purity nitrogen gas, following details given in the work Y. Liu et al. [36]. Experiments were performed at the conditions of convective diffusion (RPM = 400) using Tacussel rotating disc system.

Working electrode substrate was $(Nb\text{-}Ti)_2AlC$ cylinder, the diameter d = 6 mm and a thickness h = 5 mm, embedded in a Kel-F holder for rotating disc electrodes Tacussel and sealed with the epoxy resin, so that only front surface (0.2827 cm^2) was exposed to the solution. Before the electrochemical deposition of Pt, $(Nb\text{-}Ti)_2AlC$ substrate disks were polished on emery papers 600, 1200, 2400 and 4000, and subsequently cleaned and reduced by hydrogen evolution in 0.5 M H_2SO_4 for 10 min. at j = -0.1 A cm^{-2}. Electrochemical deposition of Pt was performed by cycling $(Nb\text{-}Ti)_2AlC$ substrate with the sweep rate of 2 mV s^{-1} from 0.0 V to -0.8 V, or -0.9 V vs. SCE immediately after immersion in the solution containing x mM K_2PtCl_4 + 0.5 M NaCl (pH 4). Three samples of electrochemically deposited Pt sub-monolayer and ultra-thin layers (corresponding to 10, 30 and 100 Pt MLs) were used for the investigation of the ORR in 0.5 M H_2SO_4.

It should be stated here that this material, along with some other MAX phases (Ti_2AlC, Ti_3SiC_2, etc.), represent one of the most stable materials in sulfuric acid [42], since the electrode passivation takes place at potentials more positive than 0.16 V vs. SCE and the increase of current density due to oxygen evolution, or MAX phase dissolution, cannot be detected up to about 2.0 V vs. SCE.

2.2. ORR investigations

ORR was investigated in 0.5 M H_2SO_4 at the room temperature using the same, standard three-electrode cell. Before the investigation of the ORR all Pt samples were cycled 20 times in 0.5 M H_2SO_4 at the room temperature from -0.25 V to 1.20 V vs. SCE with the sweep rate of 100 mV s^{-1} in order to determine the electrochemically active surface area (EASA) of each Pt layer from the charge of hydrogen desorption on the CV curves.

Procedure of the ORR investigation was as follows: Electrodes were kept in 0.5 M H_2SO_4 saturated with oxygen until stable open circuit potential was established. CVs of the ORR were recorded at six different RPMs (600, 900, 1600, 2500, 3000 and 3400) with 20 mV s^{-1} in the potential range from 0.7 V to 0.0 V vs. SCE. Only backward cycles were considered in the analysis.

2.3. Characterization of samples by XPS

The XPS analyses were carried out in a PHI VersaProbeII Scanning XPS system using monochromatic Al Kα (1486.6 eV) X-rays focused to a 100 μm spot and scanned over the area of 400 um x 400 um. The photoelectron take-off angle was 45° and the pass energy in the analyzer was set to 117.5 eV and 46.95 eV to obtain wide energy spectra and high energy resolution spectra for the C 1s, O 1s, Ir 4f and Ti 2p regions, respectively. Dual beam charge compensation with 7 eV Ar^+ ions and 1 eV electrons were used to maintain a constant sample surface potential regardless of the sample conductivity. All XPS spectra were charge referenced to the unfunctionalized, saturated carbon (C-C) C 1s peak at 284.8 eV. The operating pressure in the analytical chamber was less than $4x10^{-9}$ mbar. Deconvolution of spectra was carried out using PHI MultiPak software (v.9.8.0.19). Spectrum background was subtracted using the Shirley method.

3. RESULTS AND DISCUSSION

3.1. Electrochemical deposition of Pt on $(Nb\text{-}Ti)_2AlC$ substrate

The LSVs of Pt electrochemical deposition on $(Nb\text{-}Ti)_2AlC$ substrate, performed with the sweep rate of 2 mV s^{-1} and RPM = 400 in the solutions containing 2 mM and 3 mM K_2PtCl_4 + 0.5 M NaCl (pH 4) are presented in Fig. 1(a). If the cycling starts immediately after immersion of the rotating disc electrode ($(Nb\text{-}Ti)_2AlC$) in the solution, peaks of electrochemical deposition of Pt are well-defined, being placed at potentials more negative than about -0.25 V vs. SCE. As expected, the height of these peaks, as well as the amount of electrochemically deposited Pt, increases with the increase of the K_2PtCl_4 concentration. For 2 mM and 3 mM K_2PtCl_4 solutions, plateaus on the LSVs, corresponding to the diffusion limiting current density of hydrogen evolution on electrochemically deposited Pt, are established at about -0.45 V vs. SCE, being slightly different for both curves. Quite similar results are obtained in the work of Y. Liu et al. [36] for Pt electrochemical deposition on a rotating Au electrode. It was concluded that the commencement of H_{UPD} induces deactivation of the Pt electrochemical deposition, while at the potentials of the beginning of hydrogen evolution this process is self-terminated [36]. During the reverse (backward) sweep electrochemical deposition of Pt begins at about -0.45 V vs. SCE (when hydrogen evolution stopped) and almost identical LSV is obtained as that presented in Fig. 1(a).

In order to define the current density of electrochemical deposition of Pt, following LSVs are compared in Fig. 1(b): the LSV recorded in the solution containing 0.5M NaCl on pure substrate ($(Nb\text{-}Ti)_2AlC$) – solid black line, the LSV of electrochemical deposition of Pt recorded in the solution containing 3 mM K_2PtCl_4 + 0.5 M NaCl (pH 4) – dotted blue line and the LSV recorded in the solution containing 0.5M NaCl on electrochemically deposited Pt layer obtained from the solution 3 mM K_2PtCl_4 + 0.5 M NaCl (pH 4) – dashed red line, all of them recorded with v = 2 mV s^{-1} and RPM = 400 in the potential range from 0.0 V to -0.8 V vs. SCE. As can be seen pure substrate does not contribute to the current density for electrochemical deposition of Pt (solid black line), while certain cathodic current density of electrochemically deposited Pt recorded in 0.5 M NaCl could clearly be detected on the LSV of Pt electrochemically deposited on $(Nb\text{-}Ti)_2AlC$ from the solution 3 mM K_2PtCl_4 + 0.5 M NaCl - dashed red line). After electrochemical deposition of Pt electrode was taken out from the cell, washed and transferred in the cell with a pure supporting electrolyte (0.5 M NaCl - previously purged with nitrogen for 30 min.) where it was cycled in the same potential range. Hence, some cathodic process, most probably adsorption/desorption of Cl^- ions at potentials more positive than -0.40 V vs. SCE and HER at potentials more negative than -0.40 V vs. SCE, contributes to the total current density of electrochemical deposition of Pt.

Considering LSVs presented in Fig. 1(c) it appears that after subtracting the LSV obtained in pure supporting electrolyte (j_a) on deposited Pt film from the LSV obtained during electrochemical deposition of Pt (j_b), the value of the diffusion limiting current density amounts to about -0.10 mA cm^{-2} ($j_b - j_a$), indicating that the process of electrochemical deposition of Pt is not completely self-terminated, but its contribution could be considered as negligible. Obtained LSV for pure electrochemical deposition of Pt ($j_b - j_a$) was used for determination of limiting potentials for electrochemical deposition of 10, 30 and 100 MLs of Pt.

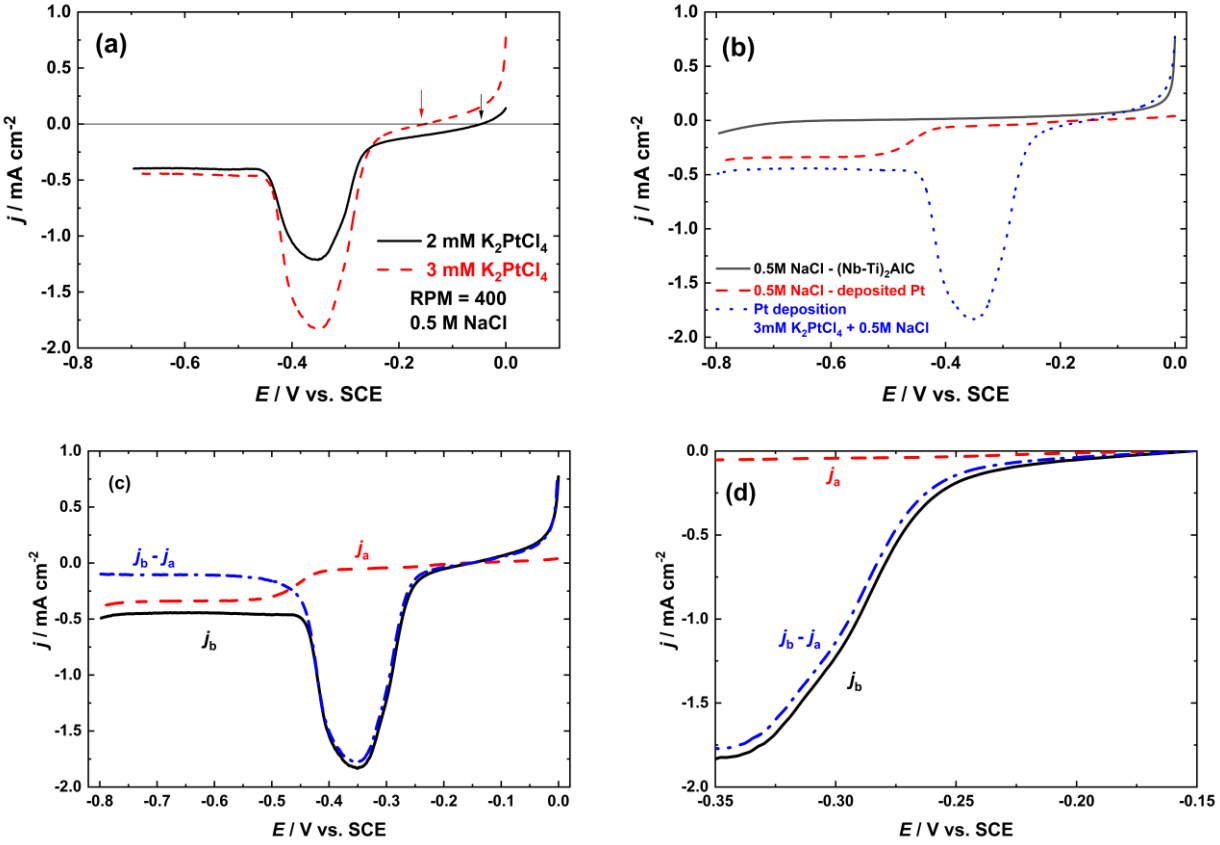

Figure 1. (a) LSVs of Pt electrochemical deposition on $(Nb\text{-}Ti)_2AlC$ substrate performed in the solutions containing 2 mM and 3 mM K_2PtCl_4 + 0.5 M NaCl (pH 4). (b) LSV recorded in the solution containing 0.5 M NaCl on pure substrate ($(Nb\text{-}Ti)_2AlC$) – solid black line, LSV recorded in the solution containing 3 mM K_2PtCl_4 + 0.5 M NaCl (pH 4) – dotted blue line and LSV recorded in the solution containing 0.5 M NaCl on electrochemically deposited Pt layer obtained from the solution 3 mM K_2PtCl_4 + 0.5 M NaCl (pH 4) – dashed red line, (c) LSV obtained by subtracting j_a from j_b (j_b - j_a) representing the LSV of pure Pt deposition: all LSVs were recorded with the sweep rate of 2 mV s^{-1} and RPM = 400.

Slika 1. (a) Krive taloženja platine na $(Nb\text{-}Ti)_2AlC$ nosaču u rastvoru: 2 mM i 3 mM K_2PtCl_4 + 0.5 M NaCl (pH 4), (b) Voltamogrami snimljeni u rastvoru 0.5M NaCl na čistom $(Nb\text{-}Ti)_2AlC$ nosaču – puna crna linija, voltamogram snimljen u rastvoru: 3 mM K_2PtCl_4 + 0.5 M NaCl (pH 4) – tačkasta plava linija i voltamogram dobijen u rastvoru 0.5M NaCl na elektrohemijski istaloženom sloju platine dobijenom iz rastvora: 3 mM K_2PtCl_4 + 0.5 M NaCl (pH 4) – isprekidana crvena linija, (c) Voltamogrami dobijeni oduzimanjem j_a od j_b (j_b - j_a) koji predstavljaju taloženje čiste platine: sve krive su snimljene pri brzini promene potencijala od 2 mV s^{-1} i brzini rotacije RPM = 400.

Taking into account statement [36] that the current efficiency for electrochemical deposition of Pt at potentials more positive than the cathodic peak potential amounts to 100 %, the amount of electrochemically deposited Pt, curve $j_b - j_a$ from Fig. 1(c) was corrected for the base line and the charge under the Pt deposition peak was obtained by integration of the j_{Pt} vs. t curve presented in Fig. 2(a), while corresponding Q_{Pt} vs. E dependence is shown in Fig. 2(b). Dividing Q_{Pt} with 295 x 10^{-6} C cm^{-2} (charge needed for a close packed Pt monolayer -111) the coverage (θ) expressed in Pt MLs was obtained and presented as a function of potential in Fig. 2(c). The charge needed for a close packed Pt monolayer was obtained as shown in our previous paper for Ir monolayer [41] using atomic radius of Pt (r_{Pt} = 1.77 x 10^{-8} cm). As can be seen during the process of electrochemical deposition of Pt from the solution containing 3 mM K_2PtCl_4 + 0.5 M NaCl (pH 4) about 420 MLs of Pt were deposited. Determined values of limiting potentials for electrochemical deposition of 10, 30 and 100 MLs of Pt are presented In Fig. 2(d).

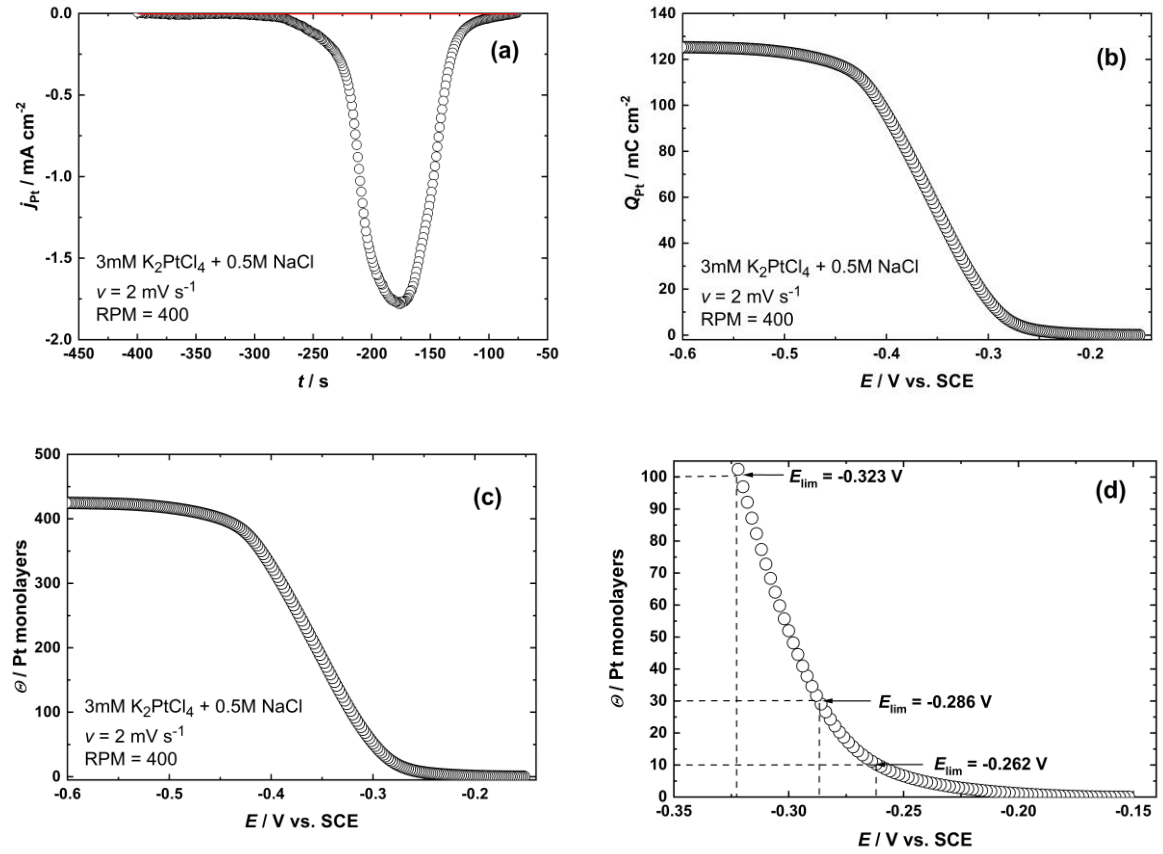

Figure 2. (a) j_{Pt} vs. t dependence after subtraction of a base line, (b) Q_{Pt} vs. E dependence and (c) θ vs. E dependence for electrochemical deposition of Pt on (Nb-Ti)$_2$AlC substrate with the sweep rate of 2 mV s^{-1} and RPM = 400, from the solution containing 3 mM K_2PtCl_4 + 0.5 M NaCl (pH 4), (d) limiting potentials for electrochemical deposition of 10, 30 and 100 MLs of Pt.

Slika 2. (a) Zavisnost j_{Pt} od t posle oduzimanj bazne linije (b) Zavisnost Q_{Pt} od E i (c) θ od E za elektrohemijsko taloženje Pt na (Nb-Ti)$_2$AlC nosaču; brzina promene potencijala 2 mV s^{-1}, brzina rotacije electrode RPM = 400, elektrolit za taloženje: 3 mM K_2PtCl_4 + 0.5 M NaCl (pH 4), (d) granični potencijali za elektrohemijsko taloženje 10, 30 i 100 monoslojeva Pt.

Considering results presented in Figs. 1 and 2, it seems reasonable to assume that by adjusting limiting value of potential (E_{lim}) to the charges necessary for 10, 30 and 100 MLs of Pt, it would be possible to obtain Pt deposits consisting of 10, 30 and 100 MLs. By expanding the coverage and potential scales in Fig. 2(c) it is possible to determine the limiting potential for electrochemical deposition of certain number of Pt MLs, as shown in Fig. 2(d). Hence, electrochemical deposition of Pt was performed from the solution containing 3 mM K_2PtCl_4 + 0.5 M NaCl (pH 4) at RPM = 400 by the LSV at the sweep rate 2 mV s^{-1} (step size 1 mV) starting at -0.05 V vs. SCE and finishing at the E_{lim} defined in Fig. 2(d).

After electrochemical deposition of Pt presented in Fig. 1(b) ($j_b - j_a$) the electrode was taken out from the cell, washed and transferred in the cell with 0.5 M H_2SO_4, previously purged with nitrogen for 30 min. The quality of Pt deposit was checked by cycling it 20 times from -0.25 V vs. SCE to 1.20 V vs. SCE with the sweep rate of 100 mV s^{-1} at RPM = 1600. The result for 20th cycle for all investigated samples is shown in Fig. 3(a). It is obvious that good quality of Pt deposit was obtained with well-defined peaks of hydrogen adsorption/desorption and peaks of Pt-oxide formation and reduction.

3.2. Electrochemical characterization of samples containing 10, 30 and 100 MLs of Pt by CV

In order to determine the electrochemically active surface area (EASA) for each sample, analysis presented in Fig. 3(b) for sample containing 10 Pt MLs has been applied for each sample. The current axis at the CV was given in

mA, while the charge corresponding to the monolayer of hydrogen desorption was obtained after correction for the double layer current, amounting to 281.1 μC. This value was divided with 210 μC cm^{-2} (charge necessary for a monolayer of hydrogen desorption from the polycrystalline Pt [43] and obtained value in cm^2 (given in the figure) was used as the EASA. Obtained values of EASA for each sample are given in Table 1. The weight (*G*) of Pt for each sample is also presented in Table 1.

Table 1. The EASA, the weight of electrochemically deposited Pt (G), the half wave potential ($E_{1/2}$).

Tabela 1- Realna površina elektrode -EASA, masa istaložene Pt-G, potencijal polutalasa ($E_{1/2}$)

No. Pt MLs	EASA/cm^2	*G*/μg cm^{-2}	$E_{1/2}$/V vs. SCE
10	1.339	2.98	0.446
30	2.182	8.94	0.453
100	3.21	29.82	0.460

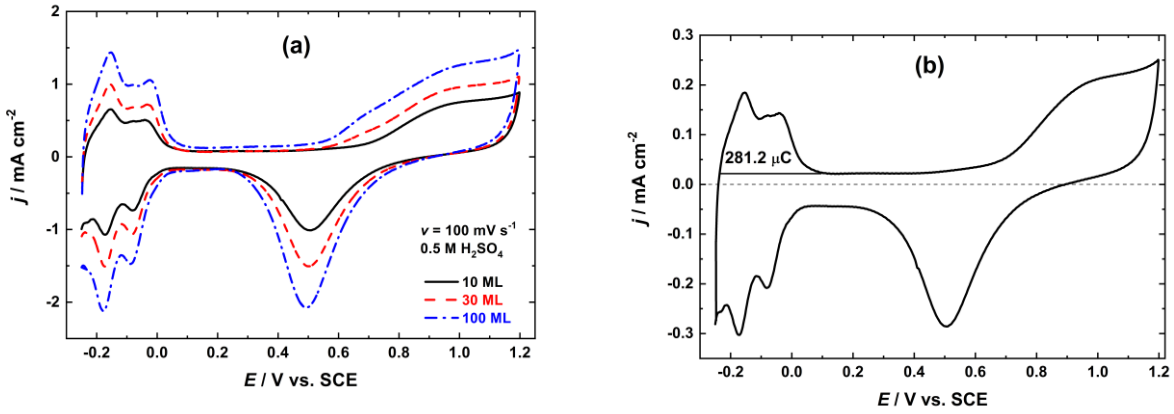

Figure 3. (a) 20th CVs recorded in 0.5 M H_2SO_4 with a sweep rate of 100 mV s^{-1} for all three samples, (b) example of the determination of $Q_{des}(H)$ for sample with 10 MLs of Pt.

Slika 3. (a) Ciklični voltamogrami (dvadeseti ciklus) snimljeni u 0.5 M H_2SO_4, brzina promene potencijala 100 mV s^{-1} za sva tri uzorka, (b) primer određivanja $Q_{des}(H)$ za uzorak sa 10 monoslojeva Pt.

3.3. Characterization of the sample with 10 MLs of Pt by XPS analysis

The XPS analysis, performed at several positions of the electrode surface, confirmed the presence of metallic Pt only (among inevitable peaks of carbon (C1s) and oxygen (O1s) impurities).

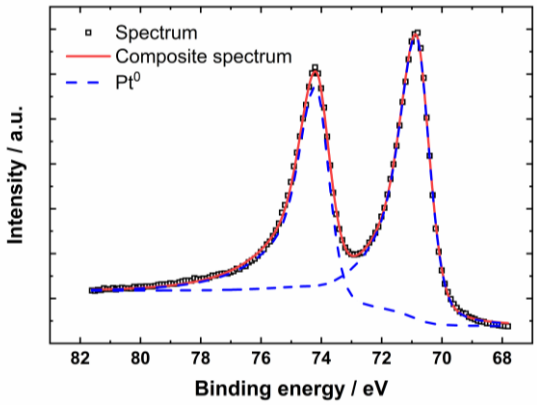

Figure 4. Result of the XPS analysis of electrochemically deposited Pt on the $(Nb\text{-}Ti)_2AlC$ substrate.

Slika 4. Rezultati XPS analize elektrohemijski istaložene Pt na $(Nb\text{-}Ti)_2AlC$ nosaču.

The XPS spectrum of Pt is presented in Fig. 4. Within the experiment geometry the information depth of analysis was about 5 nm. The Pt 4f spectrum was fitted with doublet structure ($f_{7/2}$ – $f_{5/2}$ doublet separation equals 3.3 eV) with main $4f_{7/2}$ line centered at 70.8 eV which indicate metallic state of Pt [44-46].

3.4. Investigation of the ORR at different Pt samples

After saturation of 0.5 M H_2SO_4 with oxygen, electrodes were immersed in the solution and left at open circuit potential until stable value was established (usually about 0.65 V vs. SCE). ORR was investigated by cycling electrodes from 0.65 V vs. SCE to 0.00 V vs. SCE and back with the sweep rate of 20 mV s^{-1} at RPMs of 600, 900, 1600, 2500, 3000 and 3400. Only backward sweeps were used for the analysis and they are presented in Fig. 5 for all samples. Well defined *j* – *E* responses, typical for the ORR were obtained for all samples.

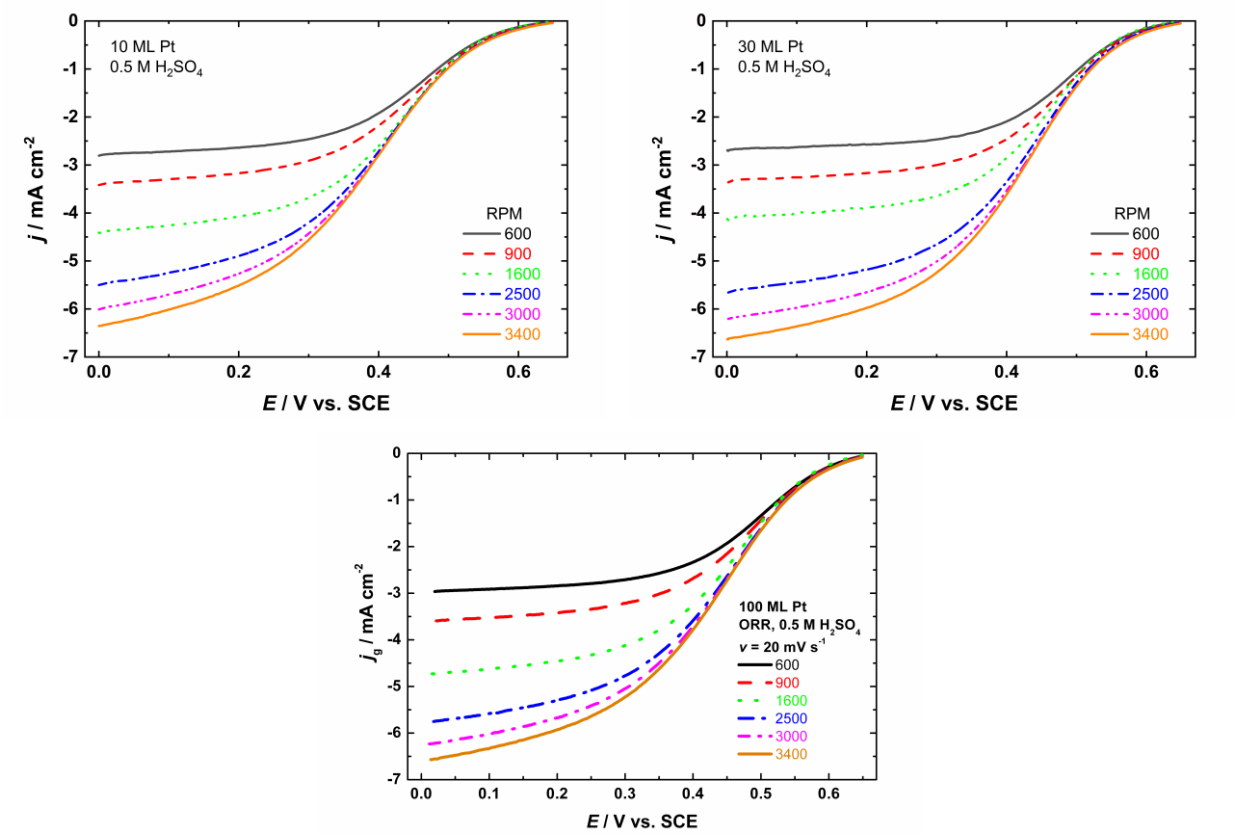

Figure 5. j - E responses for the ORR recorded at 10, 30 and 100 MLs of Pt at different RPMs (marked in the figure) with the sweep rate of 20 mV s^{-1} in 0.5 M H_2SO_4.

Slika 5. j - E zavisnosti za reakciju redukcije kiseonika snimljene na 10, 30 i 100 monoslojeva Pt pri različitim brzinama rotacije electrode; brzina promene potencijala 20 mV s^{-1} , elektrolit 0.5 M H_2SO_4.

The onset potential was found to be ~ 0.9 V vs. RHE (0.65 V vs. SCE in Fig. 5), that is in good accordance to already published literature data for ORR at Pt based catalysts in sulfuric acid solution [47]. It could be seen that in low overpotentials region, close to open circuit potential the ORR was kinetically controlled, e.g. the overall reaction rate was predominantly determined by slow electron transfer causing independence of measured current on rotation rate (Fig. 5). The experimentally recorded diffusion limiting current densities, expressed per geometric surface area, were close to the theoretically predicted ones for ORR at 1600 RPM in 0.5 M H_2SO_4 (– 4 mA cm^{-2}). The diffusion limiting current density is the function of number of electrons transferred (4 electrons for ORR at Pt in acid solutions), rotation rate and the electrolyte properties: concentration of dissolved oxygen, diffusion coefficient and kinematic viscosity at corresponding temperature, as well as geometric surface area. The experimentally obtained values of diffusion limiting current densities close to theoretically predicted ones were indication of full geometric surface area coverage, according to Mayrhofer et al. [48]. As stated earlier [48,49] the accordance of the experimentally obtained values of diffusion limiting current densities for the ORR with the theoretically calculated one for the same conditions is very important due to following factors: if the catalyst's loading is too low the rotation disc electrode cannot be completely covered; on the other side, if the loading is to high the mass transport conditions, necessary for rotating disc electrode describing equations, are no longer fulfilled [48].

Detailed analysis was performed for curves recorded at the RPM = 1600, presented for all samples in Fig. 6(a). With the increase of electrochemically deposited MLs of Pt the ORR is seen to start at more positive potentials. The values of half wave potentials ($E_{1/2}$) are given in Table 1.

The kinetic current density (j_k) was calculated by using the Koutecky−Levich equation [50] from the relation

$$j_k = \frac{j\, j_L}{j_L - j} \qquad (1)$$

where: j – current density at a chosen potentials (E = 0.35 V, 0.40 V, 0.45 V and 0.50 V) and j_L - diffusion limiting current density at E = 0.00 V vs. SCE. These values correspond to the geometric surface area of 0.2827 cm^2. The values of the kinetic current densities at chosen potentials are presented in Fig. 6(b). In order to obtain kinetic current densities corrected for the EASA the values presented in Fig. 6(b) were multiplied by the geometric surface area and divided with the EASA and corresponding results are given in Fig. 6(c). Finally, mass kinetic current densities corrected for the EASA ($j_{k(mass)}$), expressed in A g^{-1}, are obtained by dividing $j_{k(EASA)}$ with the weight of electrochemically deposited Pt (G) (Fig. 6(d)). In all cases the highest values are obtained for 10 ML of Pt, with the $j_{k(mass)}$ reaching about 820 A g^{-1} at the potential of -0.35 V vs. SCE. With the increase of electrochemically deposited Pt MLs the values of all parameters presented in Fig. 6(b,c,d) are seen to decrease.

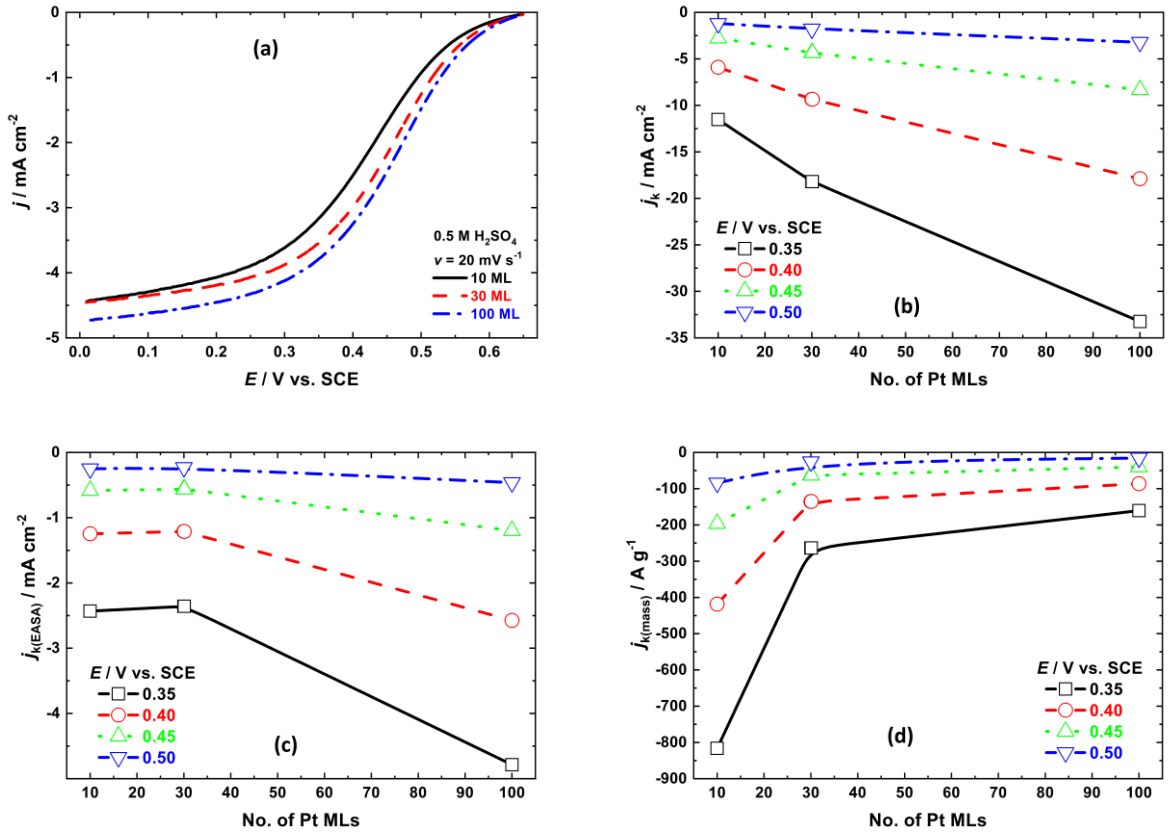

Figure 6. (a) j- E curves for the ORR at all samples recorded at RPM = 1600 and a sweep rate of 20 mV s^{-1}, (b) the kinetic current densities as a function of the number of electrochemically deposited Pt MLs, (c) the kinetic current densities as a function of the number of electrochemically deposited Pt corrected for the EASA, (d) the mass kinetic current densities as a function of the number of electrochemically deposited Pt MLs expressed in A g^{-1}.

Slika. 6. (a) j - E krive za reakciju redukcije kiseonika na svim ispitivanim uzorcima, dobijene pri brzini rotacije od RPM= 1600 i brzini promene potencijala od 20 mV s^{-1}, (b) vrednosti kinetičke gustine struje u funkciji broja elektrohemijski dobijenih monoslojeva Pt, (c) kinetičke gustine struje izražene po elektrohemijski aktivnoj površini elektrode u funkciji broja monoslojeva Pt (d) vredniosti kinetičke struje po masi Pt, A g^{-1}, u funkciji broja istaloženih monoslojeva.

However, it is common to compare ORR catalysts activities at the potentials of 0.85 V or 0.90 V vs. RHE (the potential values of practical interest for fuel cells application), where the mass transport contribution could be neglected. Since in this case sulfuric acid solution was used, which implied lower onset potential for ORR than, for instance usually used perchloric acid, the comparison should be done at 0.85 V vs. RHE (0.60 V vs. SCE in our case). The obtained results were presented in Table 2.

Tafel dependences for samples containing 10, 30 and 100 MLs are presented in Fig. 7(a) and 7(b). It could be seen that well defined dependences were obtained with two Tafel slope values: one close to −60 mV dec^{-1}, at low current densities and the other one ~ −120 mV dec^{-1} at high current densities, suggesting the same mechanism of the reaction with the transition in the Tafel slope that is related to the change in the nature of adsorbed oxygen containing species and their coverage variation with potential. These values are in good accordance to already widely accepted literature Tafel slope values for the ORR at Pt based catalysts in the same solution [51]. The change of Tafel slope is assigned to the changes of adsorption conditions for adsorbed oxygen containing species, from Temkin to Langmuir type, without changing the rate determining step [49,51].

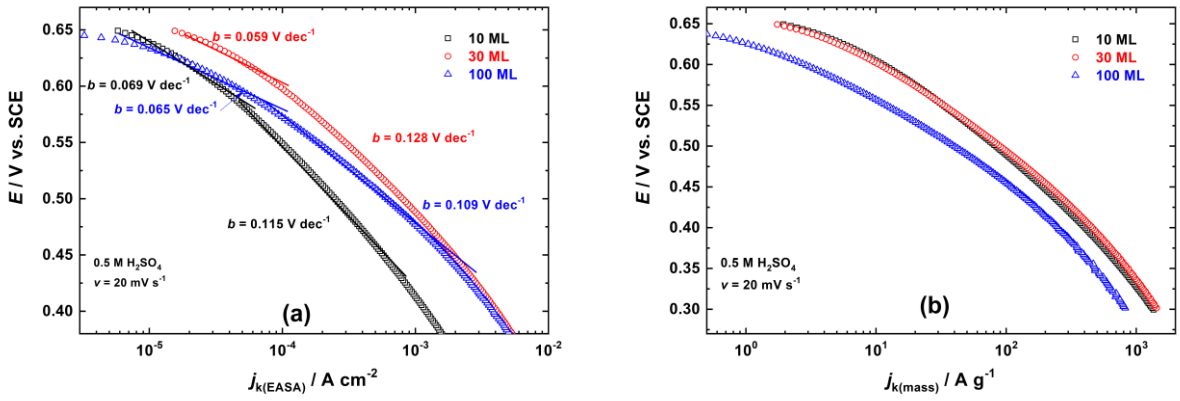

Figure 7. Tafel plots for the samples containing 10, 30 and 100 MLs Pt. (a) The kinetic current densities are normalized per electrochemically active surface area of Pt. (b)The kinetic current densities are normalized per mass of Pt loading.

Slika 7. Tafelove zavisnosti za uzorke od 10, 30 i 100 monoslojeva Pt. (a) Kinetičke gustine struje po elektrohemijski aktivnoj površini elektrode. (b) Kinetičke gustine struje izražene po masi istaložene platine.

Table 2. The comparison of the catalytic activities in terms of specific and mass kinetic current density at the constant potentials of 0.45 V and 0.60 V vs. SCE

Tabela 2. Poređenje katalitičkih aktivnosti u smislu specifične i masene kinetičke gustine struje pri konstantnim potencijalima od 0,45 V i 0,60 V u odnosu na SCE

Electrode	*E*/V vs. SCE	$j_{k(EASA)}$ / mA cm^{-2}	$j_{k(mass)}$ / A g^{-1}
10 MLs Pt	0.45	-0.64	-192.8
	0.60	-0.036	-12.9
30 MLs Pt	0.45	-1.88	-218.1
	0.60	-0.09	-10.7
100 MLs Pt	0.45	-1.58	-108.7
	0.60	-0.042	-2.85

The obtained values for kinetic current density of 0.036 mA cm^{-2} normalized to electrochemically active surface area, as well as mass activity of 12.9 A g^{-1} Pt for 10 ML Pt/(Nb-Ti)$_2$AlC at the constant potential value of 0.60 V vs. SCE (Table 2) are in good accordance to already published ones by Adzic and coworkers [47] for commercial carbon supported Pt catalyst, as well as for Pt at TiO_2 doped carbon nanotubes - Pt/c-TiO_2/CNTs-700. Namely, in above mentioned paper at the potential value of 0.80 V vs. RHE mass activities of 64 A g^{-1} for Pt/C and 39 A g^{-1} for Pt/c-TiO_2/CNTs-700 were referred. Comparing mass activity for 10 ML Pt/(Nb-Ti)$_2$AlC (37.4 A g^{-1} - Fig. 7(b)) at the potential value of 0.55 V vs. SCE (~0.80 V vs. RHE) with the one reported in Ref. [47] for Pt/C-TiO_2/CNTs-700 [47] it could be concluded that these values are almost identical.

On the other hand, obtained values for catalytic activities of 10 MLs Pt/(Nb-Ti)$_2$AlC are in good accordance to widely accepted benchmarks for oxygen reduction reaction at Pt based catalysts in acid solutions defined by Gasteiger et. al [52]. Having in mind that in Gasteiger's paper benchmarks were listed for elevated temperatures of 65 ^{o}C and 80 ^{o}C) (temperatures fuel cells working conditions) while our catalysts were tested at room temperature (25 ^{o}C) and taking into account literature reported value for the apparent enthalpy of activation for ORR in the low current density region of 60 kJ mol^{-1}, in the high current density region of 41 kJ mol^{-1} [53] it is clear that specific activity for our 10 MLs Pt/(Nb-Ti)$_2$AlC catalyst would be much higher at mentioned elevated temperatures values.

Having in mind quite good activity of the 10 Pt MLs at $(Nb\text{-}Ti)_2AlC$ support in comparison to carbon supported ones this novel catalyst could be considered as promising candidate for low temperature fuel cell application. Two facts should be emphasized here: the low cost and well-established commercial procedure for $Nb\text{-}Ti)_2AlC$ support production; electrochemical deposition has always been considered as simple and cost-effective process for catalyst preparation.

4. CONCLUSION

Thin Pt layers containing 10, 30 and 100 MLs were successfully deposited on $(Nb\text{-}Ti)_2AlC$ support. XPS analysis confirmed the presence only Pt(0) species at the surface – complete reduction of platinum to the metallic form.

These catalysts exhibited high catalytic activity for the ORR in acid solution in comparison to carbon supported ones already reported in literature at the same experimental conditions. The best ORR performance was obtained for the 10 MLs Pt. Having in mind quite good activity of the 10 Pt MLs at $(Nb\text{-}Ti)_2AlC$ support, low cost of commercial production of the support in different forms (powders of different specific surface area, plates etc..) and cheap electrochemical equipment needed for electrochemical deposition this novel catalyst could be considered as promising candidate for low temperature fuel cell application.

Acknowledgements

This work was supported by the Ministry of Education, Science and Technological Development of the Republic of Serbia (Contract No. 451-03-68/2022-14/200053 and Contract No.451-03-68/2022-14/200135). The authors would like to thank Prof. M. Barsoum, Drexel University Department of Material Science & Engineering 3141, Chestnut Street Philadelphia, PA 19104 USA, for preparation of $(Nb\text{-}Ti)_2AlC$ substrates.

5. REFERENCES

[1] K.R.Williams (1966) An Introduction to Fuel Cells, Elsevier, New York.

[2] J.M.Chapuzet, A.Lasia, J.Lessard (1998) in J.Lipkowski, P.N.Ross (Eds.), Electrocatalysis, Wiley-VCH, p155.

[3] K.Uosaki, S.Ye, H.Naohara, Y.Oda, T.Hab, T.Kondo (1997) Electrochemical Epitaxial Growth of a Pt(111) Phase on an Au(111) Electrode, J Phys Chem B, 101, 7566–7572.

[4] H.F.Waibel, M.Kleinert, L.A.Kibler, D.M.Kolb (2002) Initial stages of Pt deposition on Au(111) and Au(100), Electrochim Acta, 47,1461–1467.

[5] J.J.Whalen, J.D.Weiland, P.C.Searson (2005) Electrochemical Deposition of Platinum from Aqueous Ammonium Hexachloroplatinate Solution, J. Electrochem. Soc., 152, C738–C743.

[6] F.J.E.Scheijen, G.L.Bertramo, S.Hoeppener, T.H.M.Housmans, M.T.M.Koper (2008) The electrooxidation of small organic molecules on platinum nanoparticles supported on gold: influence of platinum deposition procedure, J. Solid State Electrochem., 12, 483–495.

[7] M.S.Zei, T.Lei, G.Ertl (2003) Spontaneous and electrodeposition of Pt on Ru (0001), Phys Chem, 217, 447–458.

[8] S.R.Brankovic, J.X.Wang, R.R.Adžić (2001) Metal monolayer deposition by replacement of metal adlayers on electrode surfaces, Surf. Sci., 47, L173–L179.

[9] M.F.Mrozek, Y.Xie, M.J.Weaver (2001) Surface-Enhanced Raman Scattering on Uniform Platinum-Group Overlayers: Preparation by Redox Replacement of Underpotential-Deposited Metals on Gold, Anal. Chem., 73, 5953–5960.

[10] M.Van Brussel, G.Kokkinidis, I.Vandendael, C.Buess-Herman (2002) High performance gold-supported platinum electrocatalyst for oxygen reduction, Electrochem. Commun., 4, 808–813.

[11] K.Sasaki, Y.Mo, J.X.Wang, M.Balasubramanian, F.Uribe, J.McBreen, R.R.Adzic (2003) Pt submonolayers on metal nanoparticles—novel electrocatalysts for H2 oxidation and O_2 reduction, Electrochim. Acta, 48, 3841–3849.

[12] J.Zhang, Y.Mo, M.B.Vukmirovic, R.Klie, K.Sasaki, R.R.Adzic (2004) Platinum Monolayer Electrocatalysts for O_2 Reduction: Pt Monolayer on Pd(111) and on Carbon-Supported Pd Nanoparticles, J.Phys.Chem.B, 108,10955–10964.

[13] Y.D.Jin, Y.Shen, S.J.Dong (2004) Electrochemical Design of Ultrathin Platinum-Coated Gold Nanoparticle Monolayer Films as a Novel Nanostructured Electrocatalyst for Oxygen Reduction, J. Phys. Chem. B, 108, 8142–8147.

[14] A.Kongkanand, S.Kuwabata (2005) Oxygen reduction at platinum monolayer islands deposited on Au (111), J. Phys. Chem. B, 109, 23190–23195.

[15] J.Zhang, F.H.B.Lima, M.H.Shao, K.Sasaki, J.X.Wang, J.Hanson, R.R.Adzic (2005) Platinum Monolayer on Nonnoble Metal−Noble Metal Core−Shell Nanoparticle Electrocatalysts for O_2 Reduction, J. Phys. Chem. B, 109, 22701–22704.

[16] Y.G.Kim, J.Y.Kim, D.Vairavapandian, J.L.Stickney (2006) Platinum Nanofilm Formation by EC-ALE via Redox Replacement of UPD Copper: Studies Using in-Situ Scanning Tunneling Microscopy, J. Phys. Chem. B, 110, 17998–18006.

[17] S.H.Yoo, S.Park (2007) Platinum-Coated, Nanoporous Gold Nanorod Arrays: Synthesis and Characterization, Adv. Mater, 19, 1612–1615.

[18] M.Shao, K.Sasaki, N.S.Marinkovic, L.Zhang, R.R.Adzic (2007) Synthesis and characterization of platinum monolayer oxygen-reduction electrocatalysts with Co–Pd core–shell nanoparticle supports, Electrochem. Commun., 9, 2848–2853.

[19] J.F.Zhai, M.H.Huang, S.J.Dong (2007) Electrochemical Designing of Au/Pt Core Shell Nanoparticles as Nanostructured Catalyst with Tunable Activity for Oxygen Reduction, Electroanalysis, 19, 506–509.

[20] S.H.Yoo, S.Park (2008) Electrocatalytic applications of a vertical Au nanorod array using ultrathin Pt/Ru/Pt layer-by-layer coatings, Electrochim Acta, 53, 3656–3662.

[21] L.Wang, S.J.Guo, J.F.Zhai, X.D.Hu, S.J.Dong (2008) Ultrathin platinum-group metal coated hierarchical flowerlike gold microstructure:Electrochemical design and characterization, Electrochim Acta, 53, 2776–2781.

[22] Y.L.Yu, Y.P.Hu, X.W.Liu, W.Q.Deng, X.Wang (2009) The study of Pt@Au electrocatalyst based on Cu underpotential deposition and Pt redox replacement, Electrochim Acta, 54,3092–3397.

[23] R.E.Rettew, J.W.Guthrie, F.M.Alamgir (2009) Layer-by-Layer Pt Growth on Polycrystalline Au:Surface-Limited Redox Replacement of Overpotentially Deposited Ni Monolayers, J. Electrochem. Soc., 156, D513–D516.

[24] S.R.Brankovic, J.McBreen, R.R.Adžić (2001) Spontaneous deposition of Pt on the Ru(0001) surface, J. Electroanal. Chem, 503, 99–104.

[25] Y.Nagahara, M.Hara, S.Yoshimoto, J.Inukai, S.H.Yau, K.Itaya (2004) In Situ Scanning Tunneling Microscopy Examination of Molecular Adlayers of Haloplatinate Complexes and Electrochemically Produced Platinum Nanoparticles on Au(111), J. Phys. Chem. B,108, 3224–3230.

[26] S.Strbac, S.Petrovic, R.Vasilic, J.Kovac, A.Zalar, Z.Rakocevic (2007) Carbon monoxide oxidation on Au(1 1 1) surface decorated by spontaneously deposited Pt, Electrochim. Acta, 53, 998–1005.

[27] J.Kim, C.Jung, C.K.Rhee, T.H.Lim (2007) Electrocatalytic Oxidation of Formic Acid and Methanol on Pt Deposits on Au(111), Langmuir, 23,10831–10836.

[28] B.Du, Y.Y.Tong (2005) A Coverage-Dependent Study of Pt Spontaneously Deposited onto Au and Ru Surfaces: Direct Experimental Evidence of the Ensemble Effect for Methanol Electro-Oxidation on Pt, J. Phys. Chem. B, 109, 17775–17780.

[29] S.Kim, C.Jung, J.Kim, C.K.Rhee, S.M.Choi, T.H.Lim (2010) Modification of Au Nanoparticles Dispersed on Carbon Support Using Spontaneous Deposition of Pt toward Formic Acid Oxidation, Langmuir, 26, 4497–4505.

[30] S.Manandhar, J.A.Kelber (2007) Spontaneous deposition of Pt and Ir on Ru: Reduction to intermediate oxidation states, Electrochim. Acta, 52, 5010–5017.

[31] K.Uosaki, S.Ye, Y.Oda, T.Haba, K.Hamada (1997) Adsorption of Hexachloroplatinate Complex on Au(111) Electrode. An in Situ Scanning Tunneling Microscopy and Electrochemical Quartz Microbalance Study, Langmuir, 13, 594–596.

[32] J.V.Zoval, J.Lee, S.Gorer, R.M.Penner (1998) Electrochemical Preparation of Platinum Nanocrystallites with Size Selectivity on Basal Plane Oriented Graphite Surfaces, J. Phys. Chem. B, 102, 1166-1175.

[33] I.Lee, K.Y.Chan, D.L.Phillips (1998) Atomic force microscopy of platinum nanoparticles prepared on highly oriented pyrolytic graphite, Ultramicroscopy, 75, 69-76.

[34] I.Lee, K.Y.Chan, D.L.Phillips (1998) Growth of electrodeposited platinum nanocrystals studied by atomic force microscopy, Appl. Surf. Sci., 136, 321-330.

[35] A.J.Gregory, W.Levason, R.E.Noftle, R.Le Penven, D.Pletcher (1995) Studies of platinum electroplating baths Part III. The electrochemistry of $Pt(NH_3)_{4-x}(H_2O)^{2+}_2$ and $PtCl_{4-x}(H_2O)^{(2-x)-}_x$,J. Electroanal. Chem., 399, 105-113..

[36] Y.Liu, D.Gokcen, U.Bertocci, T.P.Moffat (2012) Self-Terminating Growth of Platinum Films by Electrochemical Deposition, Science, 338,1327-1330.

[37] Y.Liu, C.M.Hangarter, D.Garcia, T.P.Moffat (2015) Self-terminating electrodeposition of ultrathin Pt films on Ni: An active, low-cost electrode for H2 production, Surface Science, 631, 141–154.

[38] B.M.Jović, V.D.Jović, U.Č.Lačnjevac, S.I.Stevanović, J.Kovač, M.Radović, N.V. Krstajić (2016) Ru layers electrodeposited onto highly stable Ti_2AlC substrates as cathodes for hydrogen evolution in sulfuric acid solutions, J. Electroanal. Chem., 766, 78–86.

[39] B.M.Jović, V.D.Jović, G.Branković, M.Radović, N.V.Krstajić (2017) Hydrogen evolution in acid solution at Pd electrodeposited onto Ti_2AlC, Electrochim. Acta, 224, 571–584.

[40] N.R.Elezović, G.Branković, P.Zabinski, M.Marzec, V.D.Jović (2020) Ultra-thin layers of iridium electrodeposited on Ti_2AlC support as cost effective catalysts for hydrogen production by water electrolysis, J. Electroanal. Chem., 878, 114575.

[41] N.R.Elezović, M.N.Krstajić Pajić, V.D.Jović (2020) Sub-monolayers of iridium electrodeposited on Ti_2AlC substrate as catalysts for hydrogen evolution reaction in sulfuric acid solution, Materials Protection, 61,181-191.

[42] V.D.Jovic, B.M.Jovic, S.Gupta, T.El-Raghy, M.W.Barsoum (2006) Corrosion behavior of select MAX phases in NaOH, HCl and H_2SO_4, Corrosion Science, 48, 4274-4282.

[43] S.Trasatti, O.A.Petri (1991) Real surface area measurements in electrochemistry, Pure & Appl. Chem., 63, 711-734.

[44] W.-D.Schneider, C.Laubschat (1981) Actinide---noble-metal systems: An x-ray-photoelectron-spectroscopy study of thorium-platinum, uranium-platinum, and uranium-gold intermetallics, Physical Review B, 23, 997-1005.

[45] S.Porsgaard, L.Merte, L.Ono, F.Behafarid, J.Matos, S.Helveg, M.Salmeron, B.Cuenya, F.Besenbacher (2012) Stability of Platinum Nanoparticles Supported on SiO2/Si(111): A High-Pressure X-ray Photoelectron Spectroscopy Study, Acs Nano, 6, 10743-10749.

[46] A.Arico, A.Shukla, H.Kim, S.Park, M.Min, V.Antonucci (2001) An XPS study on oxidation states of Pt and its alloys with Co and Cr and its relevance to electroreduction of oxygen, Applied Surface Science, 172, 33-40.

[47] K.Huang, K.Sasaki, R.R.Adzic, Y.Xing (2012) Increasing Pt oxygen reduction reaction activity and durability with a carbon-doped TiO2 nanocoating catalyst support, J. Mater. Chem., 22, 16824-16832.

[48] K.J.J.Mayrhofer, D.Strmcnik, B.B.Blizanac, V.Stamenkovic, M.Arenz, N.M.Markovic (2008) Measurement of oxygen reduction activities via the rotating disc electrode method: From Pt model surfaces to carbon-supported high surface area catalysts, Electrochimica Acta, 53, 3181–3188.

[49] N.R.Elezovic, P.Zabinski, P.Ercius, M.Wytrwal, V.R.Radmilovic, U.C.Lacnjevac, N.V.Krstajic (2017) High surface area Pd nanocatalyst on core-shell tungsten based supportas a beneficial catalyst for low temperature fuel cells application, Electrochimica Acta, 247, 674–684.

[50] A.J.Bard, L.R.Faulken (2001) Electrochemical Methods: Fundamental and Applications, 2nd ed., Wiley, New York.

[51] Lj. M.Vracar, D.B.Sepa, A.Damjanovic (1989) Palladium Electrode in Oxygen-Saturated Aqueous Solutions Potential Dependent Adsorption of Oxygen Containing Species and Their Effect on Oxygen Reduction, J. Electrochem. Soc.,136, 1973-1977.

[52] H.A.Gasteiger, S.S.Kocha, B.Sompalli, F.T.Wagner (2005) Activity benchmarks and requirements for Pt, Pt-alloy, and non-Pt oxygenvreduction catalysts for PEMFCs, Applied Catalysis B: Environmental, 56, 9–35.

[53] N.Wakabayachi, M.Takeichi, M.Itagaki, H.Uchida, M.Watanabe (2005) Temperature-dependence of oxygen reduction activity at a platinum electrode in an acidic electrolyte solution investigated with a channel flow double electrode, J. Electroanal. Chem., 574, 339-346.

IZVOD

REAKCIJA REDUKCIJE KISEONIKA NA ELEKTROHEMIJSKI ISTALOŽENIM TANKIM SLOJEVIMA PLATINE NA $(Nb\text{-}Ti)_2AlC$ NOSAČU

Ispitivana je reakcija redukcije kiseonika na tankim slojevima platine u 0.5 mol dm^{-3} H_2SO_4. Tanki slojevi platine – čija količina naelektrisanja odgovara 10, 30 i 100 teorijskih monoslojeva Pt su istaloženi na nosaču od $(Nb\text{-}Ti)_2AlC$. Za elektrohemijsko taloženje je korišćen rastvor 3 mM K_2PtCl_4 + 0.5 M NaCl pH = 4, u uslovima konvektivne difuzije (RPM = 400) primenom metode linearne skenirajuće voltametrije (LSV) pri brzini promene potencijala od 2 mV s^{-1}. Elektrohemijski dobijeni platinski katalizatori na pomenutom nosaču su okarakterisani metodom fotoelektronske spektroskopija X-zraka (XPS), kao i elektrohemijskim tehnikama.

Za određivanje realne elektrohemijski aktivne površine elektrode je primenjena ciklična voltametrija, integracijom ispod anodnog dela voltamograma u oblasti adsorpcije vodonika na potpotencijalima. Za ispitivanje kinetike reakcije redukcije kiseonika je korišćena metoda linearne skenirajuće voltametrije na rotirajućoj disk elektrodi. Dobijene su dve vrednosti Tafelovog nagiba, jedna približno 60 mV dek^{-1} u oblasti malih prenapetosti, a druga ~ 120 mV dek^{-1}, u oblasti većih gustina struje. Katalitička aktivnost katalizatora je poređena sa vrednostima iz literature dobijenim na platini na ugljeničim nosačima na 0.85 V prema reverzibilnoj vodoničnoj elektrodi, izražena kao kinetička gustina struje po realnoj površini electrode, ili specifična aktivnost – izražena kao kinetička gustina struje po masi platine. Pokazano je da katalizator sa 10 monoslojeva platine poseduje veoma dobru katalitičku aktivnost, posebno izraženu po masi istaložene platine.

Ključne reči: *elekrohemijsko taloženje Pt, redukcija kiseonika, sumporna kiselina.*

Naučni rad
Rad primljen: 08. 11. 2021.
Rad prihvaćen: 10. 01. 2022.
Rad je dostupan na sajtu: www.idk.org.rs/casopis